MATERIALS CHEMISTRY FRONTIERS

CCS 中国化学会 CHINESE CHEMICAL SOCIETY

ICCAS

ROYAL SOCIETY OF CHEMISTRY

REVIEW

View Article Online
View Journal | View Issue

Cite this: *Mater. Chem. Front.*, 2020, **4**, 1554

Aromatic imide/amide-based organic small-molecule emitters for organic light-emitting diodes†

Yuanyuan Qin,[ab] Guoping Li, *[a] Ting Qi *[b] and Hui Huang *[c]

Received 13th February 2020,
Accepted 16th April 2020

DOI: 10.1039/d0qm00084a

rsc.li/frontiers-materials

Organic electroluminescent materials play an important role in improving the optoelectronic performance of organic light-emitting diodes (OLEDs). Aromatic imide/amide-based organic small-molecule emitters have caught increasing attention due to their unique properties, such as strong electron-withdrawing characteristics, rigid structures and high-fluorescence quantum yields. In recent years, aromatic imide/amide semiconductors have been developed rapidly, but few reviews have been specially reported on their application in OLEDs. This study classified aromatic imides/amides into maleimide (MAI), phthalimide (PHI), naphthalimide (NAI), perylenediimide (PDI), and other imide/amide units according to their chemical structure to summarize the advances of imide/amide-based organic small-molecule emitters from the perspectives of device performance and molecular design rules over the past 20 years. The luminescence mechanism was also explored. The findings of this study might provide a constructive guide towards future exploration and promote the further development of innovative imide/amide-based emitters.

1. Introduction

Organic light-emitting diodes (OLEDs) have made significant progress since Ching Wan Tang and Steven Van Slyke used tris(8-quinolinolato)aluminium (Alq_3) as an emitter to prepare OLEDs with a brightness of up to 1000 cd m^{-2} in 1987.[1] OLEDs are favoured for their high efficiency, lightweight, flexible bending, fast response, high contrast and bright colours in display applications.[2–5] To realize the commercialization of OLEDs, designing organic electroluminescent materials plays an important role besides changing the device structure and

[a] *Green Catalysis Center, College of Chemistry, Zhengzhou University, Zhengzhou 450001, China. E-mail: liguoping@zzu.edu.cn*
[b] *School of Chemical Sciences, University of Chinese Academy of Sciences, Beijing, 100049, China. E-mail: qiting@ucas.ac.cn*
[c] *College of Materials Science and Optoelectronic Technology & CAS Key Laboratory of Vacuum Physics, University of Chinese Academy of Sciences, Beijing, 100049, China. E-mail: huihuang@ucas.ac.cn*

† Electronic supplementary information (ESI) available: The definitions of the abbreviations for material names mentioned in the review and DFT calculations. See DOI: 10.1039/d0qm00084a

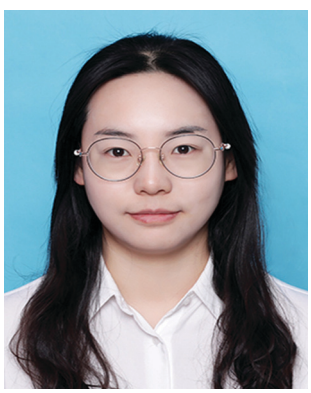

Yuanyuan Qin

Yuanyuan Qin has been a master's candidate at Zhengzhou University since 2017. In 2018, she began to study under the co-supervision of Associate Professor Ting Qi and Dr Guoping Li at the University of Chinese Academy of Sciences. Her research interests focus on the molecular design, synthesis and application of organic functional molecules in OLEDs.

Guoping Li

Guoping Li received her BS degree in 2008 from the College of Chemistry and Materials Science, Shaanxi Normal University, and her PhD degree from the Institute of Chemistry, Chinese Academy of Sciences (ICCAS), under the supervision of Prof. Hua Jiang in 2013. She then has been working in the College of Chemistry, Zhengzhou University. Her recent research interests are related to optoelectronic materials, molecular recognition and biosensors.

manufacturing process. By tuning their organic molecular structures, their properties, such as their energy gap, solubility, electron affinity and stability, can be adjusted to obtain better device performances.[6]

π-Conjugated small molecules for organic luminescent materials are widely used in OLEDs because of their simple synthesis, well-defined chemical structures, fine-tuning of energy levels, excellent reproducibility and alternative solution-based film-forming process.[7] Notably, aromatic imide/amide-based molecules as a class of important π-conjugated organic semiconductors show excellent photothermal and chemical stability, high-fluorescence quantum yields, rigid structures and good electron transmission characteristics, and are thus usually applied in optoelectronics including OLEDs,[8] organic field-effect transistors (OFETs),[9–11] and organic solar cells (OSCs).[7,12,13] In particular, the OLEDs using aromatic imide/amide-based as emitters exhibited remarkable improvement in device performances, which attracts increasing attention.

So far, reviews have been scarcely reported on the application of aromatic imide/amide-based organic small-molecule emitters in OLED devices. Therefore, the present study aimed to summarize the luminous characteristics, device performances and molecular design rules of imide/amide-based organic small-molecule emitters. Specifically, they were classified into five types according to their chemical structure, including maleimide (MAI), phthalimide (PHI), naphthalimide (NAI), perylenediimide (PDI) and other imide/amide units, to explore the progress of their applications in OLEDs in detail. The findings of this study might be helpful in providing some suggestions for the future development of aromatic imide/amide-based emitters in OLEDs. All the emitters enumerated in this study have already been applied to fabricate OLED devices.

2. Luminescence mechanism of aromatic imide/amide derivatives

The molecular structure and properties determine the luminescence mechanism, and the excited state is a key determinant in the luminescence process. In general, excited states can be divided into two types according to the positions of hole and electron orbitals before and after transition. If the distributions of electrons and holes before and after the transition are roughly the same, this is called the locally excited (LE) state. In contrast, if the electrons and holes are distributed on different fragments or different molecules before and after the transition, this is called the charge-transfer (CT) excited state. Molecules dominated by the LE state generally have the advantages of high radiative transition rates and photoluminescence efficiency and the unfavourable factor of low exciton utilization efficiency due to the difficulty of intersystem crossing.[14] In contrast, the CT state makes the electron transition lack effective orbital coupling and thus the transition moment is usually small, restricting the photoluminescence efficiency. However, the exciton binding energy is relatively weak because the distance between electrons and holes is relatively large, increasing the possibility of intersystem crossing to enhance the exciton utilization.

As a particularly important performance parameter of an OLED device, external quantum efficiency (EQE) is not only affected by the photoluminescence efficiency in the solid state, but also affected by the efficiency of production of radiative transition excitons, charge balance factor and light out-coupling efficiency. The fluorescence quantum efficiency of the emitter can reach 100%, and the charge balance factor may also get close to unity by constructing an appropriate multilayer device architecture. However, theoretically only 25% internal quantum efficiency (IQE) can be obtained according to

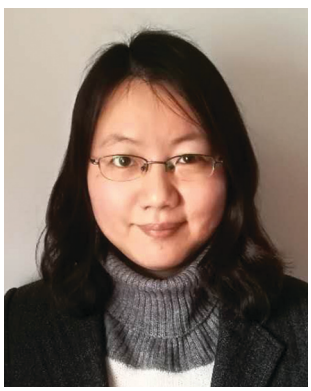

Ting Qi

Ting Qi received her PhD degree from the Institute of Chemistry, Chinese Academy of Sciences (ICCAS), in 2008. After a postdoc at the European Institute of Chemistry and Biology in France (2009–2012), she joined the School of Chemical Sciences, University of Chinese Academy of Sciences, as an associate professor in 2013. Her research presently focuses on the synthesis and applications of organic photoelectric functional materials and supramolecular assemblies.

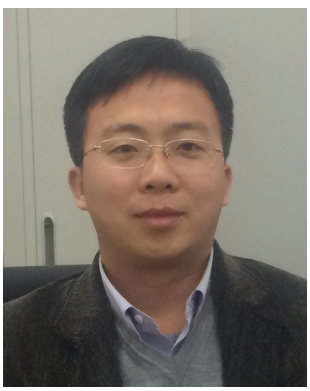

Hui Huang

Hui Huang is currently a Professor at the College of Materials Science and Opto-electronic Technologies, University of Chinese Academy of Sciences (UCAS). After ten years' experience at Dartmouth College, Northwestern University, and ConocoPhillips (Phillips 66) in the USA, he joined the UCAS in 2013. He has published over 70 peer-reviewed papers with over ten patents. His current research interests include synthesis and applications of organic/polymeric semiconductors for photovoltaics, thin-film transistors (TFTs), photodetectors, and biosensors. He was selected as an Emerging Investigator of J. Mater. Chem. A in 2017 and awarded a Distinguished Young Grant of NSFC in 2019.

the probability of production of singlet excited states in conventional fluorescent materials, so the maximum EQE (EQE_{max}) may reach about 5.5% taking the out-coupling efficiency to be 0.22.[7] To break the theoretical upper limit of quantum efficiency, an effective strategy is to improve the exciton utilization efficiency, namely, to use triplet excitons as much as possible. The current commonly used tactics for fluorescent materials are thermally activated delayed fluorescence (TADF), triplet–triplet annihilation (TTA) and hybridized local and charge-transfer (HLCT).[15–17]

The amide and imide are functional groups consisting, respectively, of one and two acyl groups as the acceptor bound to nitrogen as the donor. The whole aromatic imide/amide exhibits strong electron-withdrawing properties because of the presence of the acyl group. At present, the main core structures of aromatic imides commonly used in OLEDs are shown in Fig. 1. The density functional theory (DFT) calculations revealed that the electron and hole distributions of the representative aromatic imide/amide are roughly the same before and after the transition. That is, they are mainly locally excited. MAI mainly exhibits n–π* transition, but PHI, NAI and PDI begin to exhibit π–π* transitions as the conjugated length increases. The reason is that the energy level of the LE (π–π*) state with greater oscillator strength can be reduced when the conjugated length increases from MAI to PDI, or can be even lower than that of the LE (n–π*) state with small oscillator strength, thus increasing the fluorescence quantum yield.[18] Thus, extending the conjugated backbone of aromatic imides/amides is an efficient way to enhance luminescence efficiency.

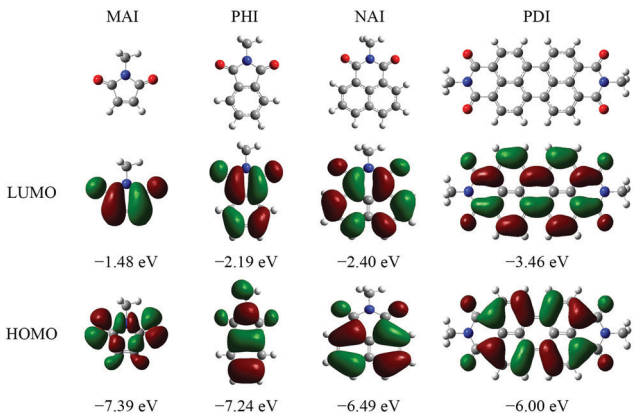

Fig. 1 Chemical structures, optimized frontier orbitals and orbital energies (eV *vs.* vacuum) of typical aromatic imides commonly used in OLEDs by DFT at the B3LYP/6-31G** level.

When constructing a D–A conjugated molecular system with an aromatic imide/amide as the acceptor, the CT state often appears. The weak binding energy of CT excitons may cause a small energy gap (ΔE_{ST}) between the singlet (S_1) and triplet (T_1) excited states. Therefore, low-energy triplet excitons can upconvert to the singlet level by a reverse intersystem crossing (RISC) process and become fluorescence emission, which can harvest both singlet and triplet excitons to achieve 100% IQE theoretically.[4,19–21] Molecules with these properties are called TADF emitters.[22] Furthermore, the weak binding energy of CT excitons can also lead to small ΔE_{ST} in high-lying CT_x states. Meanwhile, LE states exhibit an efficient radiation behaviour and a large ΔE_{ST} value. This HLCT emission process can also theoretically realize 100% exciton utilization, emitting highly efficient electroluminescence (EL) in OLEDs.[23,24]

Introducing different functional groups into molecular systems is an effective strategy to tune their molecular electronic structures so as to improve the luminescence performances of aromatic imide/amide-based emitters. The structural modification can be usually carried out at the nitrogen atom (R_1) or the aromatic core (R_2) as shown in Fig. 2. First, nitrogen atoms reduce the coupling between the aromatic backbone of the imide and the *N*-substituent (R_1), making the introduction of the substituent group (R_1) have little effect on the electronic properties of the molecule. The introduction of *N*-substituents has two advantages: (1) it alleviates the poor solubility caused by the large degree of conjugation and (2) it affects the molecular aggregation behaviour in the solid. Thus, *N*-substituents (R_1) commonly have large steric hindrance, such as alkyl chains. Second, the introduction of substituents on the aromatic core (R_2) affects its optical and electrical properties. In particular, by increasing fused aromatic rings and substituting at adjacent positions, such as 1,6,7,12-substituted PDI, the molecular structure is distorted due to the steric hindrance effect, greatly affecting the conjugation of molecules to change their electronic structures. Commonly, conjugated π-systems with a D–π–A or D–A backbone architecture

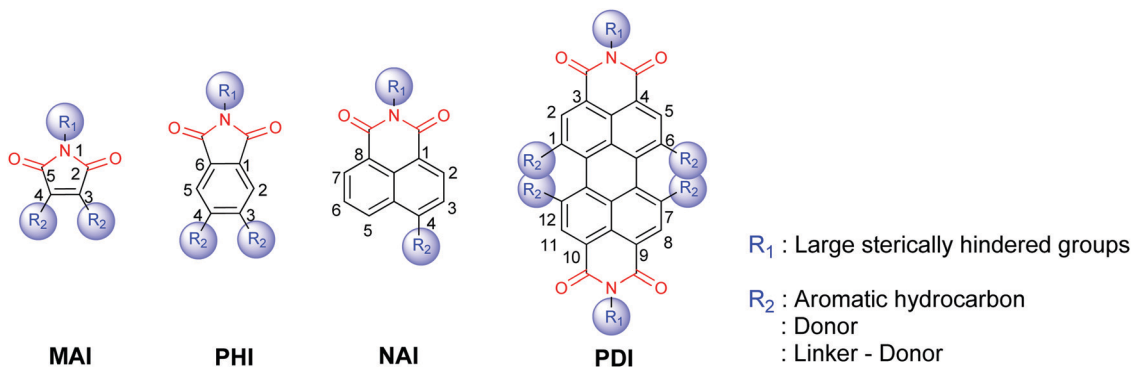

Fig. 2 Typical chemical structure modification of aromatic imide/amide-based emitters.

are constructed to improve charge balance and device efficiency by introducing different electron-donating groups into the aromatic core and using the strong electron-withdrawing characteristics of imides/amides. The conjugated D–π–A or D–A system was found to tune the bandgap and enhance charge carrier mobility, and even obtain TADF properties through structural regulation to enhance the quantum efficiency.

To date, aromatic imides/amides have been extensively used as the acceptor units of OLED emitters, which is attributed mainly to (but not limited to) the following important factors. (a) Strong electron-withdrawing properties are beneficial to the strong interchain interaction and thus enhance intramolecular charge transport. (b) The rigid planar structure of an imide/amide as the electron-withdrawing part in push–pull scaffolds facilitates the charge separation between the highest-occupied molecular orbital (HOMO) and the lowest unoccupied molecular orbital (LUMO). (c) The strong electron-withdrawing power of the imide/amide group enables molecules to have lower LUMO levels to facilitate electron injection and stabilize them. (d) Aromatic imides/amides have excellent photochemical stability and high-fluorescence quantum yields. (e) Aromatic imides/amides are well accessible to be modified by associating with electron-withdrawing or electron-donating substituents to show a hypsochromic and bathochromic shift, achieving panchromatic spectra.

3. Application of aromatic imide/amide emitters in OLEDs

3.1 MAI-based emitters

MAI is the smallest aromatic imide unit with a conjugated structure as the emitter in OLEDs. Different aryl substituents can be introduced at C(3) and C(4) to form a series of MAI derivatives (Fig. 3). In 2003, Chiu *et al.* prepared MAI-1a, MAI-1b, MAI-1c and MAI-1d by incorporating two indole groups.[25] The formation of amorphous phases with high glass-transition temperatures causes an emission of red light from such compounds in solids, proving that bisindolylmaleimide derivatives can be used as effective red emitters in OLEDs. Typical devices configured as ITO/NPB/dye/TPBi/Mg:Ag showed turn-on voltages (V_{on}) of 2–4 V, maximum luminances (L_{max}) of 1800–2400 cd m^{-2} at about 13 V and EQEs of 0.3–0.5%. The Commission Internationale de l'Eclairage (CIE) colour coordinates are located within a range of (0.61–0.63, 0.36–0.38), which is very close to that of pure red.

Afterwards, Lee and co-workers synthesized six kinds of asymmetric indolylmaleimide derivatives with different aryl substituents at the 3,4-positions, namely, MAI-2a, MAI-2b, MAI-2c, MAI-2d, MAI-2e and MAI-2f.[26] The spectroscopic properties of the asymmetric MAI derivatives are consistent with those of the symmetric ones, and the red emission is a CT from the indole–maleimide chromophore. The devices based on MAI-2f performed the best, which exhibited an optimal 1.1% EQE, along with an L_{max} close to 10 000 cd m^{-2}.

For the functionalization of MAI, a D–π–A structure is usually formed by introducing electron-donating groups such as arylamine. In the beginning, Chen's research group synthesized a non-doped glassy-red emitter (MAI-3) by introducing two naphthylphenylamino groups.[27] A simple trilayer OLED device with an ITO/MAI-3/BCP/TPBi/Mg:Ag structure was fabricated with CIE colour coordinates of (0.66, 0.32) comparable with the standard red colour. The device achieved an L_{max} close to 8000 cd m^{-2} and an EQE_{max} of 2.4%. This is the first red non-doped OLED based on red-emissive molecular materials with respectable efficiency and brightness. This research group then conducted an in-depth investigation of the performance of the non-doped red device.[28] In the presence of the hole-blocking layer BCP, the device emits pure red EL and it is essentially voltage-independent. The red non-doped device was fabricated

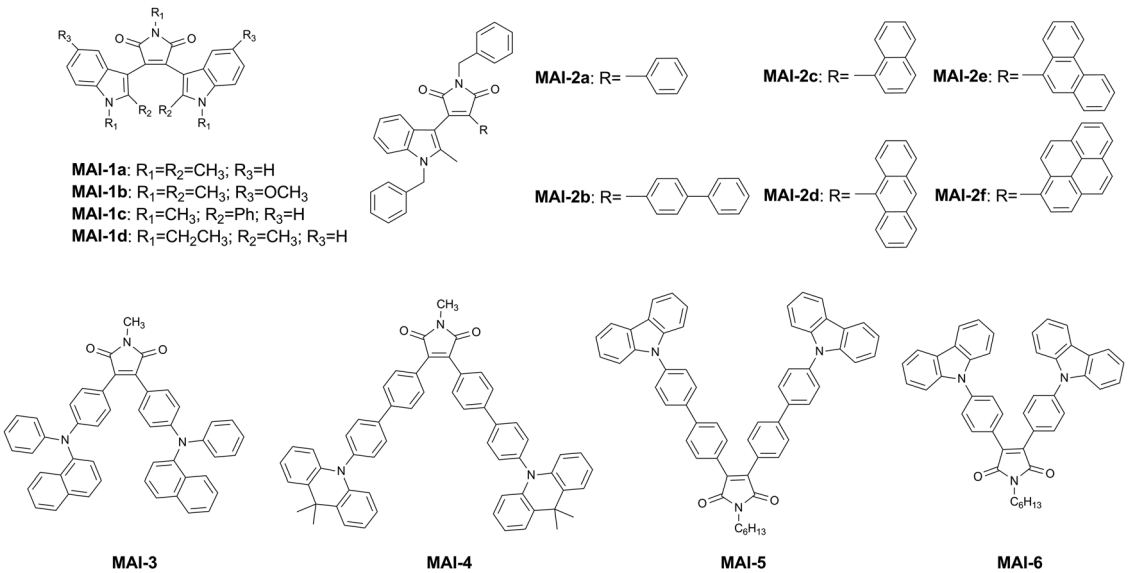

Fig. 3 Chemical structures of MAI-based emitters for OLEDs.

with an ITO/NPB (5 nm)/MAI-3 (30 nm)/BCP (20 nm)/Alq_3 (40 nm)/Mg:Ag structure, showing a high EQE of 1.6%.

In 2015, Jang *et al.* reported an emitter (MAI-4) in which an MAI acceptor was connected to a 9,9-dimethylacridan (DMAC) donor through a diphenyl bridge.[29] The absolute photoluminescence quantum yields (PLQYs) of 6 wt% MAI-4:CBP films were determined to be 42% ± 1%. The device structure was ITO/α-NPD (35 nm)/mCBP (5 nm)/6 wt% MAI-4:mCBP (20 nm)/TPBi (65 nm)/LiF (0.8 nm)/Al (100 nm), exhibiting an EL emission at 581 nm and an EQE_{max} of 1.4%.

Similarly, in 2016, Sharma *et al.* reported a highly fluorescent material (MAI-5) containing a carbazole donor.[30] MAI-5 had a high PLQY of 0.84 in solution, while the PLQY in the film form decreased obviously because of the strong concentration quenching of fluorescence in the solid state. A multilayer device configured as ITO/NPD (40 nm)/10 wt% MAI-5:CBP (15 nm)/TPBi (40 nm)/LiF (1 nm)/Al was fabricated, which achieved an EQE of 2.5% with an emission peak at 550 nm in the yellow region of the visible spectrum. MAI-5 was stable at high current density and had minimum efficiency roll-off.

In 2018, on the basis of MAI-5, Venkatramaiah *et al.* replaced the diphenyl bridge with a phenyl bridge to prepare MAI-6.[31] In comparison with emission spectra in solution, MAI-5 showed red-shifted emission (~32 nm) in the solid state, while MAI-6 exhibited blue-shifted emission (~35 nm and 71 nm). Meanwhile, MAI-6 showed a unique aggregation-induced blue-shifted emission due to the restricted intramolecular rotation process, along with aggregation-induced emission (AIE) enhancement. The device structure was ITO/NPB (40 nm)/10 wt% MAI-5 or MAI-6:CBP (15 nm)/TPBi (40 nm)/LiF (0.7 nm)/Al (100 nm), displaying EQEs of 3.7 and 4.1 with a maximum current efficiency (CE_{max} = 13.8 cd A^{-1}) for MAI-5 and MAI-6, respectively. MAI-6 displayed a very low roll-off efficiency and an L_{max} of 73 915 cd m^{-2}.

Although some MAI-based emitters can display high quantum efficiency in solution, their device performances are universally not ideal, especially due to their low EQE. This is mainly due to their small π-extended imide structural system.

3.2 PHI-based emitters

PHI is the benzene ring fusion on the MAI backbone to increase the degree of conjugation and realize the regulation of luminescence properties. Recently published studies[29,32–35] showed that emitters based on PHI were mainly constructed according to the D–A structure endowed with TADF properties. The structural design can be tuned by the introduction of substituents on the nitrogen atom and the benzene ring.

For the decoration on the benzene ring, the 3,4-disubstituted derivatives were mainly designed (Fig. 4). Similar to the MAI-based molecule MAI-6, PHI-1 was prepared by introducing a π-bridged carbazole donor into the benzene ring.[28] Using the same device structure as MAI-6, the device based on PHI-1 showed an L_{max} of 39 568 cd m^{-2}, a CE_{max} of 6.4 cd A^{-1} and an EQE of 2.6% with bright sky-blue light. The EL performance of PHI-1 was lower than that of MAI-6, which might be mainly due to the higher electron injection barrier. In addition, the incomplete separation of electron densities between the HOMO and LUMO for PHI-1 did not allow it to have a TADF behaviour because of small torsional angles at both carbazole units and the PHI moiety.

On the one hand, it is feasible to adjust the donor structure to obtain TADF properties. By replacing the carbazole donor with the DMAC donor on the basis of the same D–π–A system as PHI-1, PHI-2 exhibited obvious green TADF emission.[29] Compared with MAI-4 with different acceptors, PHI-2 still showed a much smaller ΔE_{ST} of 0.01 eV and a higher PLQY (50% ± 1%) in a 6 wt%-PHI-2:mCBP film. The device structure based on the PHI-2 film was the same as MAI-4, displaying an EL emission at 530 nm and a respectable EQE of 11.5%.

On the other hand, modifying π-bridged linking could also fine-tune the molecular electronic structure. For example, the molecular frameworks of PHI-3a and 3b were constructed by removing the benzyl linker from PHI-1 and connecting two carbazole groups directly to the benzene ring of PHI to increase the torsional angle of the donor substituent.[32] The effective separation of HOMO–LUMO electron densities led to small ΔE_{ST}s of 0.06 and 0.03 eV for PHI-3a and PHI-3b, respectively, and a small overlap of the HOMO–LUMO electron densities led to high PLQYs of 38% and 28% for neat films of PHI-3a and PHI-3b, respectively. As expected, they displayed good TADF properties. The fluorescence quantum yields in co-doped films increased to 72% and 67% for PHI-3a and PHI-3b, respectively. Multilayer OLEDs with ITO/HAT-CN (10 nm)/TAPC (30 nm)/mCBP (10 nm)/PHI-3a (8 ± 1 wt%) or PHI-3b (5 ± 1 wt%):mCBP (25 nm)/TmPyPB (45 nm)/LiF (0.9 nm)/Al (90 nm) structures were fabricated. The devices achieved CE_{max} and maximum power efficiency (PE_{max}) of up to 66.2 cd A^{-1} and 56.2 lm W^{-1} for PHI-3a and up to 66.8 cd A^{-1} and 51.2 lm W^{-1} for PHI-3b, respectively. These two devices based on PHI-3a and PHI-3b emitted yellow-green EL and exhibited high EQE values of up to 23.3% and 21.1% with CIE colour coordinates of (0.32, 0.55) and (0.37, 0.56), respectively.

Adopting a similar D–A structure, the additional chiral group 1,2-diaminocyclohexane was continuously introduced to prepare PHI-4R and PHI-4S on the basis of PHI-3a in 2018, endowed with circularly polarized luminescence (CPL) properties. These materials were the first CP-OLED emitters based on TADF characteristics.[33] The enantiomers were found to have up to 98% PLQY in co-doped films and a small ΔE_{ST} value of 0.06 eV. Moreover, the TADF enantiomers showed mirror-image circular dichroism (CD) and CPL activities and opposite circularly polarized electroluminescence signals with the dissymmetry factor (g_{EL}) values of -1.7×10^{-3} and 2.3×10^{-3}, respectively. The CP-OLED devices had ITO/HAT-CN (10 nm)/TAPC (25 nm)/TCTA (10 nm)/mCBP (10 nm)/PHI-4R or PHI-4S (15 wt%):mCBP (20 nm)/TmPyPB (45 nm)/Liq (1 nm)/Al (90 nm) structures, which achieved high EQE values of up to 19.7% and 19.8% for the two enantiomers, respectively.

Recently, given the donor substitution on the nitrogen atom, TADF and AIE were integrated to design the compound PHI-5 using carbazole as the donor and PHI as the acceptor.[34] The PLQY value of PHI-5 in solids was significantly higher than 20%.

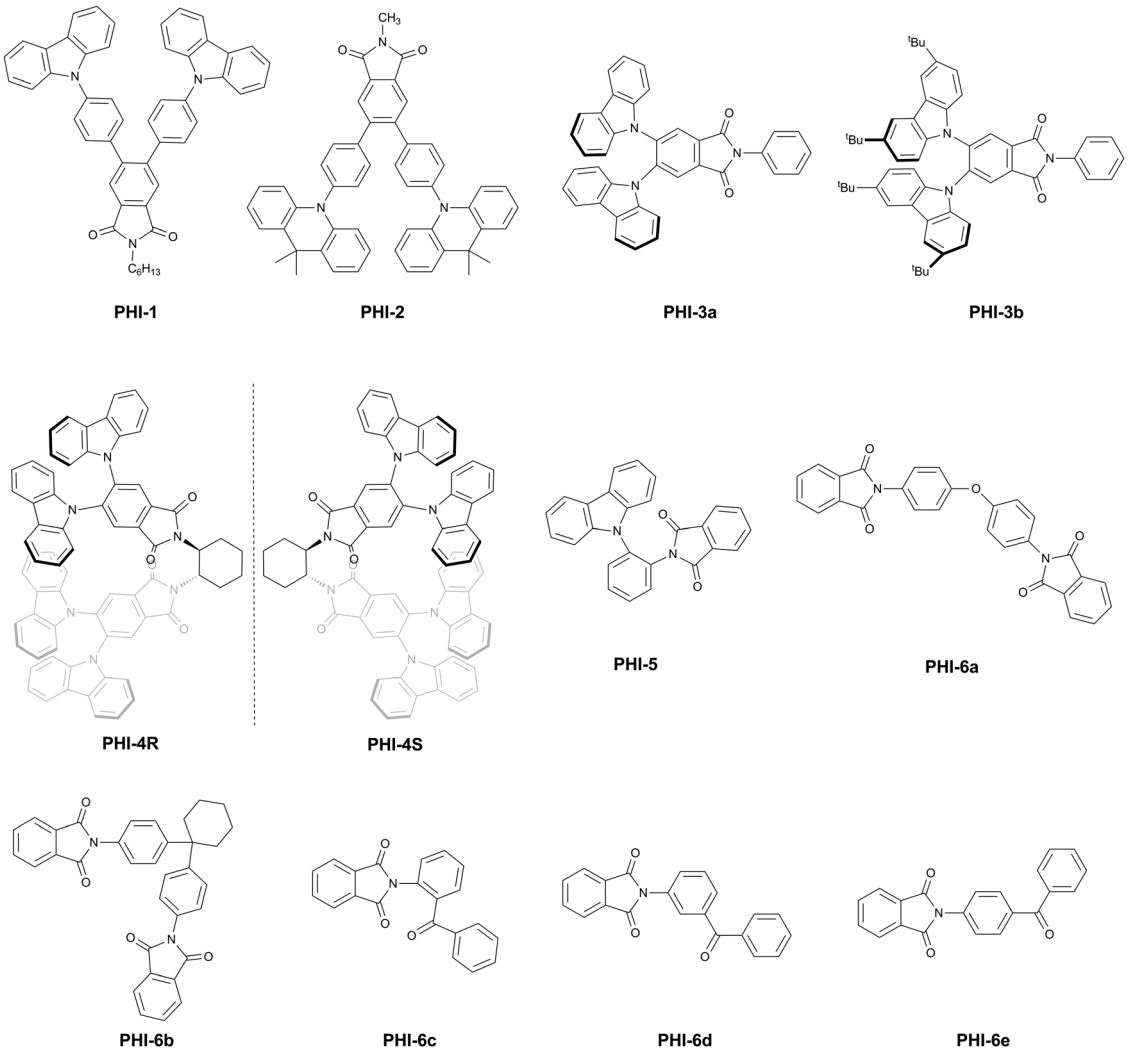

Fig. 4 Chemical structures of PHI-based emitters for OLEDs.

The main reason was that the distance between the carbon atom of the carbonyl group and the nitrogen atom of the carbazole in PHI-5 was short (3.227 Å), resulting in efficient CT through space caused by n → π* interaction between the unoccupied orbital of the carbon atom and the free electron pair of the nitrogen atom. From the spectra of the films of PHI-5 in mCP, the ΔE_{ST} was estimated to be 0.03 eV for PHI-5. The OLED configured as ITO/MoO_3 (1 nm)/NPB (20 nm)/TCTA (20 nm)/mCP (10 nm)/PHI-5 (10%, 30 nm)/TSPO1 (10 nm)/TPBi (40 nm)/LiF (0.5 nm)/Al showed an EQE_{max} of 2.4%, a CE_{max} of 6.6 cd A^{-1} and a PE_{max} of 4.0 lm W^{-1}.

In addition, Chapran *et al.* reported five exciplex-forming materials based on PHI (PHI-6a, PHI-6b, PHI-6c, PHI-6d and PHI-6e, Fig. 4), taking advantage of its powerful electron-withdrawing properties and also by substituting on the nitrogen atom.[35] These PHI-based molecules as electron acceptors were coupled with mCP, CBP, PVK and TCTA as electron donors to develop a series of different exciplex systems endowed with TADF properties, emitting sky-blue, green and red lights. All PHI derivatives showed high triplet levels around 3.1 eV. A *para*-substituted PHI-benzophenone (PHI-6e) showed the best exciplex-forming properties in a mixture with mCP, emitting sky-blue light with a PLQY of 26% and a singlet–triplet energy splitting of 0.06 ± 0.03 eV. The device structure was ITO/NPB (20 nm)/TCTA (10 nm)/mCP (5 nm)/mCP:PHI-6e (20 nm)/TmPyPB (50 nm)/LiF (1 nm)/Al (100 nm), showing an EQE_{max} of 2.9% and a brightness of 2500 cd m^{-2} at 12 V.

According to the results of some recent studies, PHI showed higher EL efficiency than MAI, which could be attributed to the following: (1) PHI has a higher conjugation degree compared with MAI and (2) its more rigid structure makes it easier to design TADF materials by the fine adjustment of its molecular structure.

3.3 NAI-based emitters

1,8-NAI possesses a more π-extended conjugation structure containing a naphthalene ring, displaying excellent luminescence properties. NAI derivatives are good film-forming luminophores as EL materials. NAI derivatives are one of the most commonly reported types of aromatic imide/amide building blocks so far used as emitters in OLEDs (Fig. 5).

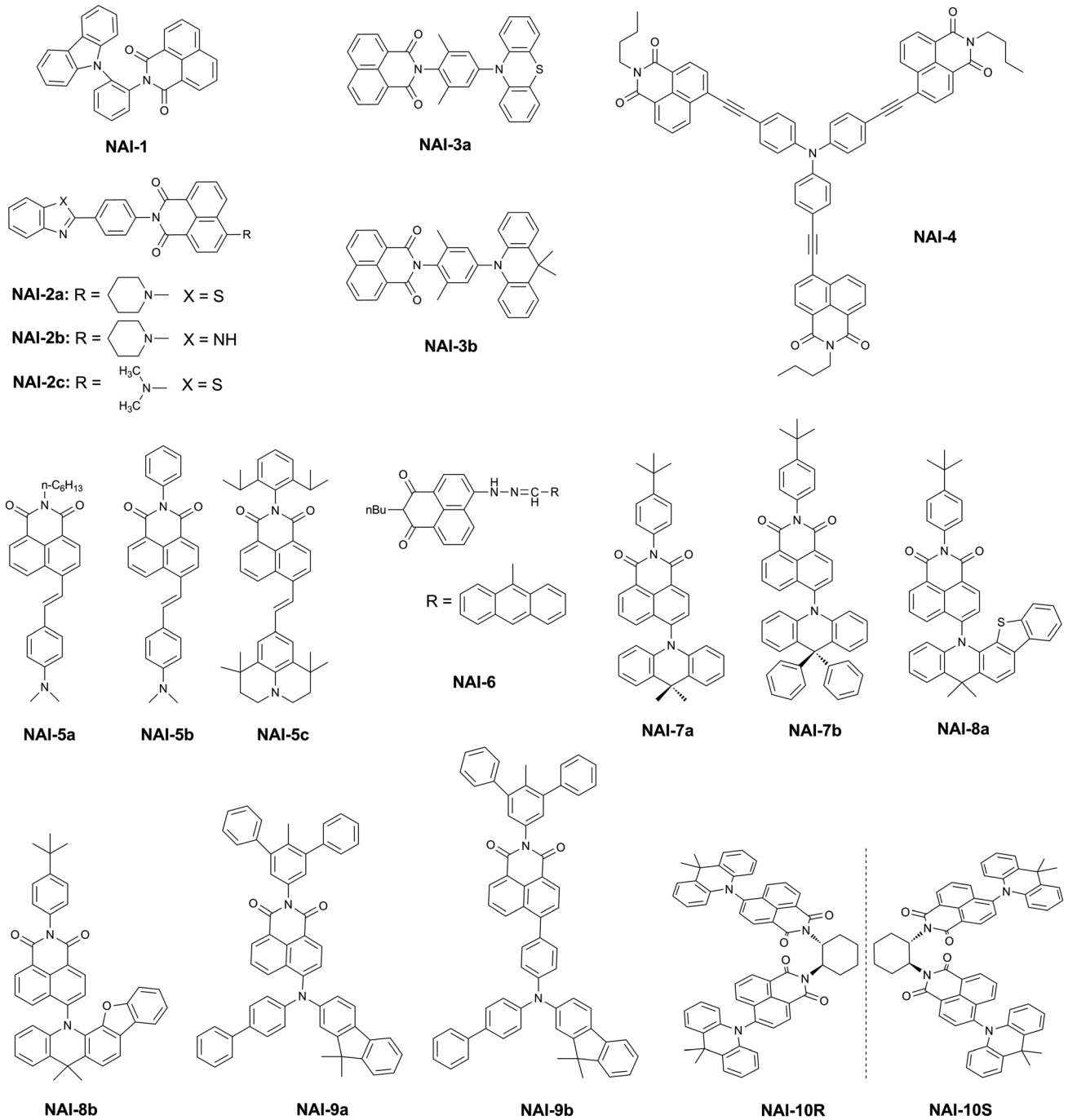

Fig. 5 Chemical structures of NAI-based emitters for OLEDs.

Their molecular structure design was based mainly on the architecture of the D–A system because of its more refined adjustment for molecular electronic characteristics. Among them, substitution on the nitrogen atom is seldom adopted. Like NAI-1, similar to PHI-5, the D–π–A structure was formed by introducing an *N*-substituted π-bridged carbazole.[34] However, the PLQY value of the NAI-1 solid sample was negligible, much lower than that of PHI-5. This might be ascribed to inefficient CT through space and a low localized triplet level.

Also, Ding *et al.* synthesized NAI-2a, NAI-2b and NAI-2c by introducing benzyl-bridged benzothiazole or benzimidazole as the electron-transporting unit considering the substitution at the N end.[36] The optimal non-doped device structure was ITO/NPB (75 nm)/NAI-2a (65 nm)/Mg:Ag/Ag (100 nm), emitting green-yellow and green EL with an L_{max} of 4500 cd m^{-2} and a CE_{max} of 0.65 cd A^{-1}. The results confirmed that the introduction of large sterically hindered groups on the N atom did not change the molecular conjugation degree and the emission colour of the original chromophore, but favoured the formation of a stable amorphous state.

Even though most studies indicated that N-terminal substituents exerted little influence on the molecular electronic structure, Wu *et al.* recently reported that the introduction of *N*-substituents resulted in emission with AIE and TADF properties. The two D–π–A architecture emitters NAI-3a and 3b were synthesized with 10-*H*-phenothiazine or DMAC as the electron donor, 2,6-dimethylphenyl as the π-bridge, and NAI as the electron acceptor.[37] Due to the steric hindrance of the π-bridge, NAI-3a and 3b both exhibited a twisted structure to limit the intermolecular motions in the solid state. Therefore, they all displayed typical AIE characteristics and red emissions with high solid-state PLQYs (55% and 39%). In addition, the twisted structures effectively separated their HOMO–LUMO electron distributions, thereby achieving smaller ΔE_{ST} values (0.05 and 0.13 eV) to realize TADF properties. The device structure was ITO/PEDOT:PSS (40 nm)/mCP (20 nm)/CBP: NAI-3a or 3b (15 nm, 12% doping)/TPBi (40 nm)/LiF (1 nm)/Al (120 nm). The NAI-3b-based device exhibited an orange EL peak at 570 nm, while the NAI-3a-based device exhibited a red EL emission at around 635 nm. The EQE_{max}s of NAI-3a and 3b reached 7.13 and 5.38%, respectively. The results demonstrated that the modification of the nitrogen atom could adjust the luminescence color and luminescence properties by constructing a twisted D–π–A structure.

Decorating the naphthalene ring with different donor substituents may be a general and efficient way to construct a D–A or D–π–A structure to obtain high luminous efficiency. Commonly, only mono-substitution happens at the 4-position due to the simplicity of the synthesis. Using the D–π–A system, Xiao *et al.* reported a starburst orange-red emitter, NAI-4, that contained triphenylamine as the electron-donating core, acetylenes as the bridges and NAI electron acceptors as the pendant branches.[38] Devices with a high doping concentration of PVK were prepared with ITO/PVK:NAI-4 (20 wt%) (70 nm)/BCP (*x* nm)/Alq_3 (30 nm)/LiF (0.5 nm)/Al (100 nm) structures. They showed L_{max}, CE_{max} and CIE coordinates of 6600 cd m^{-2}, 4.57 cd A^{-1} and (0.59, 0.40), respectively.

In 2015, Luo *et al.* prepared standard-red EL materials, NAI-5a, 5b and 5c, using an aromatic amine as the donor, ethylene-1,2-dicyl as the π-bridge and NAI as the acceptor.[39] Introducing large groups on the N atom can inhibit intermolecular interactions, and large electron-donating groups in the aromatic region can promote redshift. NAI-5a and 5b showed PLQYs of 0.51 and 0.50 with maximum emission at 669 nm and 672 nm in dichloromethane, respectively, and NAI-5c showed a PLQY of 0.45 with maximum emission at 680 nm in chloroform. The authors adopted CzPhONI as the host material that could produce an effective energy transfer process with NAI-5a, 5b and 5c due to their well-matched energy levels. Guest–host composite device structures were ITO/MoO_3 (1 nm)/TCTA (40 nm)/CzPhONI:NAI-5a, 5b and 5c (*x* wt%) (20 nm)/TPBi (45 nm)/LiF (1 nm)/Al (80 nm). With NAI-5c as the guest dopant (4 wt%), the standard-red OLED device was obtained with CIE coordinates of (0.67, 0.32), exhibiting EQE_{max} and CE_{max} of 1.8% and 0.7 cd A^{-1}, respectively. This report described the first standard-red OLED device based on NAI derivatives.

In a D–A system, all molecules are derived from 4-amino NAI to form amino conjugation, which can result in a redshift of the spectra. Initially, Gan *et al.* prepared an NAI derivative (NAI-6) by introducing the 9-anthryl substituted Schiff base moiety into the 4-amino group of NAI, emitting orange-red light.[40] The device structure based on NAI-6 as a non-doped emissive layer was ITO/CuPc (12 nm)/NPB (30 nm)/NAI-6/sodium stearate (2 nm)/Al (100 nm). The device had an EL peak at 620 nm with an L_{max} of 15.5 cd A^{-1} and a maximum current density of 2.9 mA cm^2, avoiding the concentration quenching effect of fluorescence.

In 2018, in the same way, Zeng and his colleagues reported two orange-red TADF emitters, NAI-7a and NAI-7b, by modifying the naphthalene ring to form a D–A structure.[8] The two compounds exhibited similar LUMO levels of ≈ −3.0 eV, while the HOMO level of NDI-7b (−5.52 eV) was lower than that of NAI-7a (−5.41 eV) because the quasi-planar structure of acridine was bent by the highly steric hindrance of the diphenyl groups. The ΔE_{ST} values of NAI-7a and NAI-7b were calculated to be 0.09 eV and 0.17 eV, respectively, which was conducive to an effective RISC process. In addition, their effects on emitting dipole orientations were studied, and both exhibited preferentially horizontal emitting dipole orientations in the host to boost the optical outcoupling efficiencies and consequently the EQEs of the devices. Notably, NAI-7b was less subject to concentration quenching and maintained similar PLQYs of 71.8–78.9% with doping concentrations of 1.5 wt% to 24 wt%, which were much better than those of NAI-7a. Multilayer OLEDs with ITO/MoO_3 (2 nm)/TAPC (70 nm)/mCP (10 nm)/mCPCN:*x* wt% TADF dopants (20 nm)/3TPYMB (70 nm)/LiF (0.5 nm)/Al structures were fabricated at an optimal doping concentration of 1.5 wt% for NAI-7a and 6 wt% for NAI-7b, respectively. Both devices exhibited a low V_{on} of ≈3.0 V, and an orange-red EL peaking around 597 nm and 584 nm for NAI-7a and NAI-7b, respectively. The CE_{max}, PE_{max} and EQE_{max} based on NAI-7a and NAI-7b were 50.7 cd A^{-1} and 76.2 cd A^{-1}, 53.1 lm W^{-1} and 79.7 lm W^{-1}, and 23.4% and 29.2%, respectively. The NAI-7b emitter exhibited the state-of-the-art device performance for orange-red TADF OLEDs without using any optical outcoupling technology.

Likewise, in 2019, the same research group prepared NAI-8a and NAI-8b by incorporating benzofuran and benzothiophene into the donor unit of NAI-7a and realized the adjustment of the emission colour from orange-red to pure red.[41] NAI-8a and NAI-8b had almost the same LUMO levels as the model compound NAI-7a, but they had different HOMO levels, namely −5.38 eV for NAI-8a, −5.46 eV for NAI-8b and −5.41 eV for NAI-7a, which might be due to the inductive effect of the electronegative oxygen atom and the electron-donating effect of the benzothiophene unit. The ΔE_{ST} values of NAI-8a and NAI-8b were 0.07 eV and 0.16 eV, respectively, which facilitated an efficient RISC process. The device structures of NAI-8a and NAI-8b were consistent with that of NAI-7a. The maxima of the EL spectra for the two devices were 641 nm (red) and 590 nm (orange) with CIE coordinates of (0.62, 0.38) and (0.54, 0.45), respectively. When using the optimal doping concentration

(1.5 wt%), the NAI-8a-based device achieved an EQE_{max} of 9.2%, which was much lower than that (20.3%) of the NAI-8b-based device. The poor device performance of NAI-8a could be ascribed to its much lower PLQY compared with NAI-8b, because the sulphur atom as a heavy atom compared with the oxygen atom might increase the intersystem crossing. Compared with NAI-7a, NAI-8a and NAI-8b exhibited a less-efficient RISC process, which might be attributed to the influence of their fused heterocycle groups. Inspiringly, the introduction of fused heterocycles could regulate the electron-donating ability of donors and promote the redshift of the emission wavelength, which was important for the preparation of red and deep-red emitters. Besides this, both devices suffered from severe efficiency roll-off because of the dominant triplet–triplet or singlet–triplet annihilation. Meanwhile, the EQEs of these devices gradually decreased with the increase in the doping concentration, which might be because of concentration quenching.

Introducing the AIE effect into a molecular system is one of the most efficient methods to suppress concentration quenching and exciton annihilation. For example, two D–A type emitters NAI-9a and NAI-9b with simultaneous TADF and AIE features were designed, employing a central NAI acceptor core and arylamine donor units.[42] Different from the D–A structure of NAI-9a, NAI-9b formed a D–π–A structure by inserting the phenyl linker, leading to a spatially twisted structure and better separation of HOMO and LUMO electron densities. Thus, the ΔE_{ST} value of NAI-6b (0.12 eV) was smaller than that of NAI-9a (0.15 eV). The absolute PLQY values for the neat films were 26% and 55% for NAI-9a and NAI-9b, respectively, and both NAI-9a and NAI-9b showed typical AIE activity. Multilayered OLEDs were fabricated with ITO/HAT-CN (15 nm)/TAPC (40 nm)/TCTA (5 nm)/*x* wt%-emitter:CBP (20 nm)/TmPyPB (40 nm)/LiF (1 nm)/Al (100 nm) configurations. The non-doped OLED device based on NAI-9a displayed red emission with a peak at 628 nm and CIE coordinates of (0.64, 0.35), which were close to the National Television Standards Committee's standard red (0.67, 0.33). The doped OLEDs with a doping concentration of 5 wt% offered EQE_{max}s of 4.80% and 7.59% for NAI-9a and NAI-9b, respectively. Notably, NAI-9b showed lower efficiency roll-off compared with NAI-9a because of its enhanced RISC process. In particular, in non-doped devices, the EQE roll-off of NAI-9b was nearly zero.

Introducing chiral groups into the molecular backbone of a highly efficient emitter is one of the most efficient strategies to achieve CPL, such as PHI-10R and PHI-10S. Based on the previously reported NAI-7a with high luminescence performance, Wang *et al.* prepared a pair of enantiomers (NAI-10R and NAI-10S) by linking a chiral group, 1,2-diaminocyclohexane.[43] Enantiomers with a small ΔE_{ST} of 0.07 eV showed their excellent TADF properties and stable chiroptical properties. The luminescence dissymmetry factor ($|g_{lum}|$) was calculated to be 9.2×10^{-4}. Moreover, doped OLEDs based on enantiomers as the emitters were fabricated with optimized device configurations of ITO/HAT-CN (10 nm)/TAPC (30 nm)/TCTA (5 nm)/CBP (5 nm)/PHI-10R or 10S (6 wt%):CBP (25 nm)/TmPyPB (50 nm)/LiF (0.9 nm)/Al (90 nm), which exhibited an orange-red emission with high EQE_{max}s of 12.4% and 12.3% for the two enantiomers, respectively.

As described earlier, NAI, as a planar rigid acceptor unit, may be favourable to the separation of the electron densities between the HOMO and LUMO in the push–pull molecular system, and has a good triple-state yield.[44] Therefore, NAI is extensively used in TADF emitters as an acceptor unit. In addition, the emission bands of NAI derivatives can be fine-tuned from blue to red by substitution in the naphthalene ring or nitrogen atom with diverse electron-withdrawing or electron-donating groups, indicating that NAI can be used to realize full-colour emission. In particular, for long-wavelength emitters, functionalized naphthalimide has been shown to be a promising orange or red EL material.

3.4 PDI-based emitters

PDI contains two imide units fused with the perylene ring, which is the most π-extended conjugation structure among the series of aromatic imide emitters. Therefore, for modification on the aromatic ring, four substituted positions exist in the bay area of perylene (1,6,7,12-positions, Fig. 6). PDI shows a very high-fluorescence quantum yield in solution, which is almost close to 1, but the solid-state luminescence is not ideal[45,46] mainly because of the severe aggregation-caused quenching (ACQ) effect of PDI. Research studies based on PDI derivatives focused mainly on the inhibition of the ACQ effect.[47,48]

The common way to limit ACQ is to append large sterically hindered groups to 1- or 1,7-positions of the perylene core. For example, Kozma *et al.* prepared PDI-1a and PDI-1b by introducing aromatic naphthalene and acenaphthene substituents at the 1,7-positions, respectively.[49] The substituents limited the intermolecular π–π interactions in the solid state due to their highly sterically hindered effects while preserving an extended conjugation between the substituents and the PDI core, which reduced the ACQ phenomenon to provide red emission with high PLQYs of 38% and 23% in the films of PDI-1a and PDI-1b, respectively. The device structure of PDI-1b with the more planar acenaphthene substituent was ITO/PEDOT:PSS/PVKc/PDI-1b/PF-PEG/Ba/Al, which achieved emission in the deep-red region and an EQE of 0.638%. This method has achieved the best efficiency of deep-red emission for devices based on PDI derivatives to date.

In 2018, Zong *et al.* tried to integrate the AIE effect to hinder the ACQ phenomenon, but the result was not ideal. They prepared six PDI derivatives PDI-2a, 2b, 2c, 2d, 2e and 2f by introducing three different twisted aromatic substituents at the 1- and 1,7-positions, respectively, which realized the adjustment from ACQ to AIE.[50] PDI-2e and 2f were AIE-active due to the introduction of a 4-(2,2-diphenyl-vinyl)-phenyl group. Meanwhile, the six emitters showed red, even deep-red, emission in their EL spectra. The optimal solution-processed OLED structure was ITO/PEDOT:PSS (40 nm)/CBP:1 wt% PDI-2 (40 nm)/TmPyPB (40 nm)/Liq (1 nm)/Al (100 nm). Notably, the EL performance of AIEgens PDI-2e and 2f was inferior to that of ACQgens PDI-2a, 2b, 2c and 2d. This could be ascribed to the highly twisted substituents in PDI-2e and 2f that might affect the carrier mobility, resulting in an inferior device performance. The PDI-2c-based device exhibited the best performance, with an EQE_{max} of 4.93%

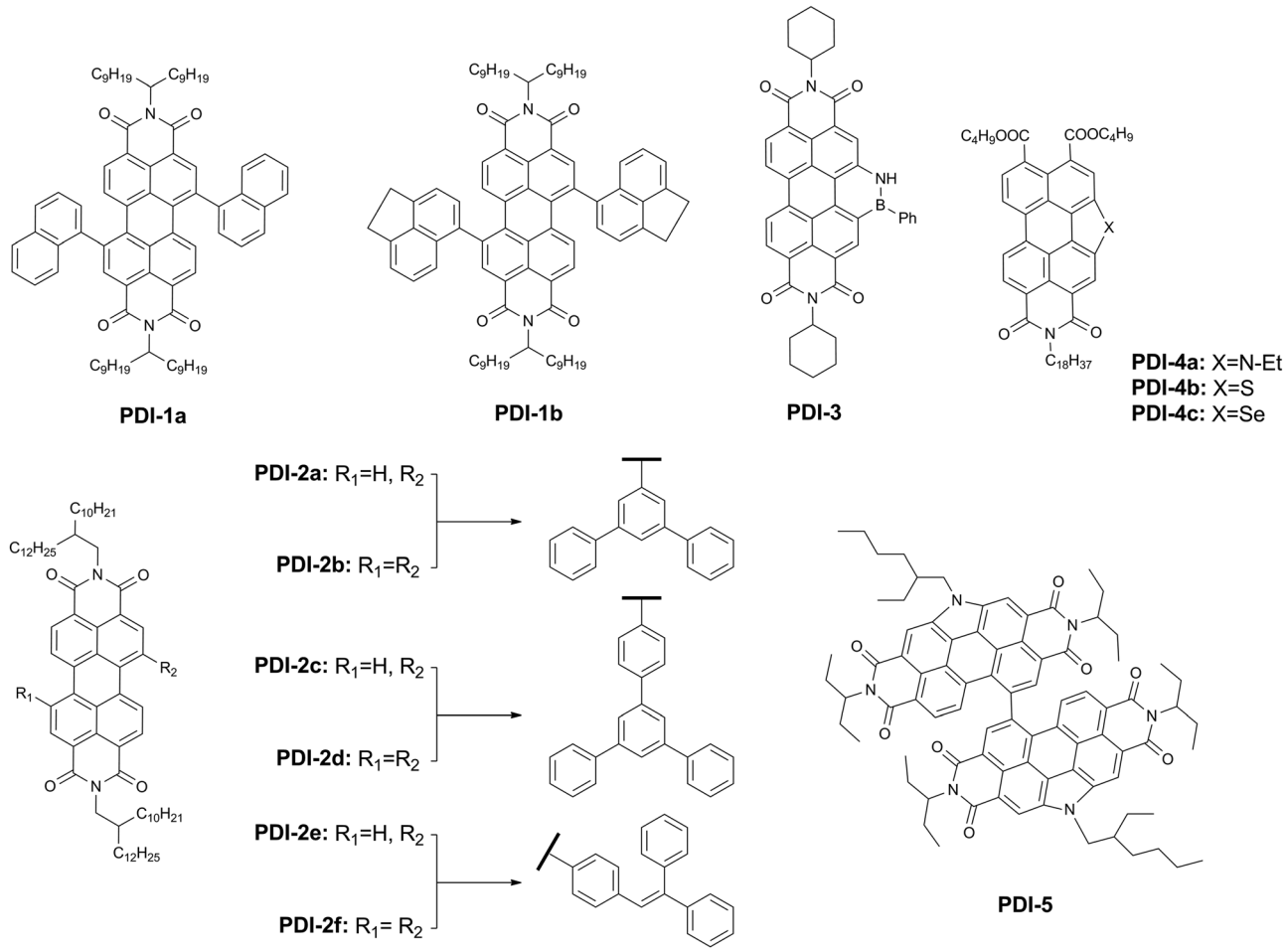

Fig. 6 Chemical structures of PDI-based emitters for OLEDs.

that approached the theoretical limit of 5.0%. It was one of the best solution-processed among the fluorescent red OLEDs.

Furthermore, heteroatom bay-annulated PDI on the 6,7-positions is expected to enhance molecular luminescence efficiency. Its unsymmetrical structure may not only improve molecular solubility but also fine-tune electronic properties. In 2015, Li *et al.* designed and synthesized the first BN-fused polycyclic aromatic hydrocarbons with a highly electron-deficient aromatic diimide (PDI-3).[51] OLEDs configured as ITO/MoO_3 (2 nm)/TCTA (80 nm)/CBP:*x* wt% PDI-3 (20 nm)/TPBi (40 nm)/LiF (1 nm)/Al (200 nm) were fabricated. When the doping proportion of PDI-3 in the CBP host was 1%, 5%, 10%, 15% and 100%, the maximum EQE was 1.57%, 1.19%, 1.01%, 0.91% and 0.05%, respectively, and the emission peak was 616, 630, 636, 646, and 682 nm, respectively.

Later on, Gupta *et al.* synthesized a series of bay-annulated perylene ester imides PDI-4a, PDI-4b and PDI-4c, only consisting of one imide unit and N, S, Se-fused heterocycles, respectively.[52] The fluorescence quantum yields of these three PDI derivatives in solution were 0.89, 0.7 and 0.06, respectively. Using PVK as the host, the devices were found to exhibit dual emission from both PVK and PDI-4 by partial Förster resonance energy transfer from PVK to the emissive dopant. Interestingly, adopting different electron-transport layers (ETLs) resulted in various electron injection barriers, thus making it possible to fine-tune the emission contribution from PVK. Eventually, the PVK doped PDI-4b and PDI-4c with TPBi as an ETL presented near-white light emission, which provided a way to achieve white light emission.

Recently, a red-light emitter (PDI-5) based on an *N*-annulated perylenediimide dimer has been proposed by Dayneko *et al.*[53] The OLED structure fabricated by all-solution processing was glass/ITO/PEDOT:PSS/PFO:PDI-5/LiF/Ag. When the PFO : PDI-5 ratio was 2 : 18, the solution-processed OLED device prepared by slot-die coating exhibited the best performance with a V_{on} of 2.6 V, an LE_{max} of 0.05 cd A^{-1}, a PE of 0.03 lm W^{-1} and an EQE of 0.06%. The emission wavelength was 635 nm. In addition, the feasibility of manufacturing OLEDs on a large scale was proved by roll–roll compatible coating.

To sum up, three common methods are available to enhance luminescence performance. The first is to introduce conjugated groups with large steric hindrance on the imide/amide core. The second is to couple with the AIE effect. The third is to incorporate heteroatoms into the extended PDI backbone, such as boron, nitrogen, and sulphur. Additionally, PDI-based OLEDs can display pure red EL, and PDI with multisubstituted

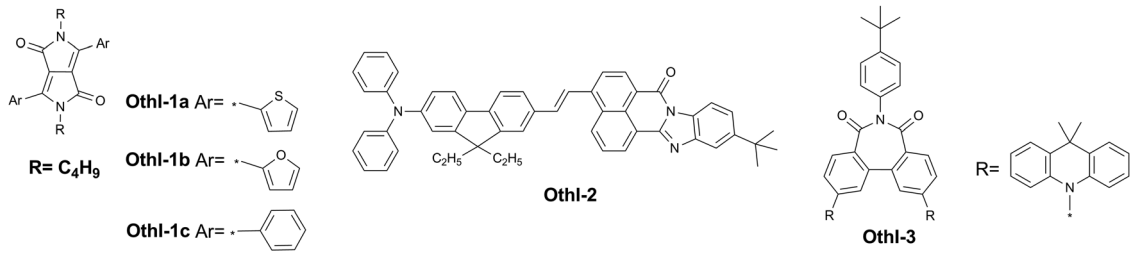

Fig. 7 Chemical structures of other imide/amide-based emitters for OLEDs.

positions can be rendered soluble in a range of both polar and non-polar solvents. Thus, the PDI chromophore is an excellent and promising building block to construct new emitters for solution-processed red OLEDs. However, PDI derivatives nearly show relatively low OLED device performance, mainly due to their large conjugated structures, which are inclined to induce an ACQ process.

3.5 Other aromatic imide/amide-based emitters

Besides the aforementioned series of aromatic imide emitters for OLEDs, a lot of other types of aromatic imides or amides are widely applied in other optoelectronic devices. These aromatic imides or amides may have great potential as building blocks of emitters in OLEDs. For example, devices based on a class of amide compounds, diketopyrrolopyrrole (DPP) derivatives, as acceptors, exhibited excellent performances in OFETs[54] and OSCs.[55,56] Data *et al.* first reported DPP derivatives (OthI-1a, 1b and 1c, Fig. 7) as emitters applied in OLED devices.[57] Three DPP derivatives achieved high quantum yields in the range of 0.69–0.79. The devices were fabricated with ITO/NPB (40 nm)/*x*% OthI-1:TAPC or CBP (30 nm)/TPBi (20 nm)/BCP (20 nm)/LiF (1 nm)/Al (100 nm) structures. The device efficiency was improved by ''diluting'' the DPP compounds in the TAPC or CBP hosts, and the EQEs could be further increased by manufacturing exciplex-enhanced OLED devices, with EQEs higher than 12% for OthI-1b, but only 0.2% for pure compounds.

Another amide compound, 7*H*-benzimidazo[2,1-*a*]benzo[*de*]isoquinolin-7-one, derived from 1,8-NAI, possesses a more extended conjugated system. Based on this skeleton, Wang *et al.* designed one red D–π–A emitter, OthI-2 (Fig. 7), exhibiting an AIE effect.[58] In addition, NAI derivative 4CzTNA was constructed as a new host material for the OthI-2 emitter. The device had an ITO/NPB (30 nm)/CBP (2 nm)/4CzTNA:OthI-2 (6 wt%) (20 nm)/Bphen (40 nm)/Mg:Ag (200 nm) structure, with an L_{max} of 6250 cd m^{-2} and a CE_{max} of 3.13 cd A^{-1}. The device efficiency was higher than that of Alq_3 as the host material, because of the much better energy transfer efficiency between 4CzTNA and OthI-2. After that, Zhou *et al.* made adjustments on the basis of 4CzTNA and prepared another NAI derivative, CzPhONI, as the host material blended with OthI-2.[59] The $^3\pi\pi^*$ state was low-lying than the ^{3}CT state of the host material, indicating that it had triplet-fusion DF (TFDF) properties. An orange-red doped device was fabricated with an ITO/MoO_3 (10 nm)/NPB (35 nm)/TCTA (10 nm)/OthI-2:CzPhONI (6 wt%, 30 nm)/TPBi (40 nm)/LiF (0.8 nm)/Al structure. The EQE_{max} value was up to 3.59%, which was much higher than its theoretically limited 25% singlet production (EQE_{max}: 2.50%). Therefore, more highly efficient OLEDs could be achieved through the molecular design strategy of host materials coupled with the harvesting method of triplet excitons.

Recently, Huang *et al.* synthesized the D–A–A compound OthI-3 with 1,1′-biphenyl-2,2′-dicarboximide (BPI) as the acceptor unit and DMAC as the donor unit (Fig. 7).[60] BPI, a novel heptagonal imide acceptor, had a balanced rigidity and rotatability, which restricted the excessive intramolecular rotation to enhance the radiative transition rate and inhibited intermolecular π–π stacking to reduce the aggregation-caused exciton quenching. The emitter exhibited aggregation-induced delayed fluorescence (AIDF) characteristics and a high PLQY (95.8%) of a neat film. The non-doped OLED configured as ITO/TAPC (25 nm)/TCTA (8 nm)/OthI-3 (35 nm)/TmPyPb (55 nm)/LiF/Al achieved a further improved EQE_{max} of 24.7%. It is the non-doped OLED device with the best performance at present.

4. Conclusions

With increased attention, functionalized imide/amide-based OLEDs have achieved encouraging device performances (Table 1). Recent studies on aromatic imide/amide-based emitters of organic small molecules have shown that they exhibited great potential in OLEDs, specifically manifesting in four main aspects. First, the diversity of substitution on an aromatic imide or amide skeleton enabled its structure to be variable, which could be used to fine-tune its molecular interactions, electronic properties and film-forming morphology. The most universal and feasible strategy was to construct a D–A/D–π–A system by appending the donor to the aryl ring and attaching the large steric group to the nitrogen atom. Second, aromatic imides/amides with a moderate conjugation core, such as NAI, BPI and PHI, could display excellent luminescence characteristics. A small conjugation core, such as MAI, could decrease the radiative transition rate to reduce the fluorescence intensity, while a large conjugation core, such as PDI, could enhance intermolecular π–π interactions to induce ACQ. Third, aromatic imide/amide-based emitters had excellent advantages acting as orange-red and red luminescent materials. The EQEs based on NAI derivative emitters exceeded 20% with a red emission, and the highest EQE was up to 29.2% with an orange-red emission. Finally, non-doped OLEDs based on an imide emitter achieved a

Table 1 Photoluminescence and electroluminescence characteristics of representative imide/amide-functionalized organic small-molecule emitters

Emitter	λ_{max} (nm)	PLQY (%)	V_{on} (V)	CE (cd A^{-1})	PE (lm W^{-1})	EQE (%)	CIE (x, y)	ΔE_{ST} (eV)	Ref.
MAI-1a	627–650[a]	—	3.0[d]	—	—	0.29[d]	(0.61, 0.38)[d]	—	25
MAI-1b	627–650[a]	—	3.9[d]	—	—	0.30[d]	(0.62, 0.37)[d]	—	25
MAI-1c	627–650[a]	—	3.6[d]	—	—	0.35[d]	(0.63, 0.36)[d]	—	25
MAI-1d	627–650[a]	—	2.0	—	—	0.54	(0.61, 0.38)	—	25
MAI-2a	630[a]	2.9[a]	6.5	0.80	0.16	0.68	(0.40, 0.29)	—	26
MAI-2b	634[a]	4.9[a]	4.5	0.87	0.24	0.6	—	—	26
MAI-2c	620[a]	7.5[a]	1.11	1.11	0.31	0.67	(0.65, 0.34)	—	26
MAI-2d	627[a]	6.8[a]	4.5	1.05	0.30	0.72	—	—	26
MAI-2e	617[a]	2.1[a]	4.5	0.83	0.29	0.54	—	—	26
MAI-2f	634[a]	23.1[a]	4.0	1.09	0.30	1.08	(0.59, 0.41)	—	26
MAI-3	683[a]/651[b]	21[a]	—	1.5	0.9	2.4	(0.66, 0.32)	—	27
MAI-3	—	—	7.5	—	—	1.6	(0.67, 0.33)	—	28
MAI-4	559[c]	42[c]	—	—	—	1.4	—	—	29
MAI-5	548[a]/580[b]	84[a]/26[b]	5.0	3.14	1.78	2.5	(0.17, 0.57)	0.8	30
MAI-6	626[a]/591[b]	42[a]/66[c]	5.85	13.8	—	4.1	(0.44, 0.51)	—	31
PHI-1	548[a]/481[b]	78[a]/70[c]	5.81	6.4	—	2.6	(0.21, 0.36)	—	28
PHI-2	517[c]	50[c]	—	—	—	11.5	—	0.01	29
PHI-3a	555[a]/530[b]/530[c]	12.7[a]/38[b]/84.1[c]	3.8	66.2	56.2	23.3	(0.32, 0.55)	0.06	32
PHI-3b	533[a]/545[b]/547[c]	24.9[a]/28[b]/69.5[c]	4.0	66.8	51.2	21.1	(0.37, 0.56)	0.03	32
PHI-4R	515[a]/533[b]/528[c]	18.0[a]/41[b]/79.8[c]	3.4	59.0	53.0	19.7	—	0.06	33
PHI-4S	515[a]/533[b]/528[c]	18.0[a]/41[b]/79.8[c]	3.4	59.4	52.9	19.8	—	0.06	33
PHI-5	517[a]/514[b]	1[a]/20[b]	4.9	6.6	4.0	2.4	(0.23, 0.41)	0.03	34
PHI-6e	497[c]	26[c]	5.0	4.9	2.2	2.9	(0.24, 0.41)	0.06	35
NAI-2a	521[a]	80[a]	10[d]	0.65[d]	0.12[d]	—	(0.43, 0.53)[d]	—	36
NAI-2b	518[a]	77[a]	7[d]	0.94[d]	0.26[d]	—	(0.37, 0.57)[d]	—	36
NAI-2c	512[a]	54[a]	6[d]	0.56[d]	0.12[d]	—	(0.38, 0.57)[d]	—	36
NAI-3a	624[b]	55[b]	6.0	16.8	9.3	7.13	(0.59, 0.40)	0.05	37
NAI-3b	595[b]	39[b]	5.0	12.4	5.2	5.38	(0.37, 0.42)	0.13	37
NAI-4	—	—	6.5	4.57	—	—	(0.59, 0.40)	—	38
NAI-5a	634[a]/678[b]/622[c]	62[a]/1[b]/29[c]	—	—	—	—	—	—	39
NAI-5b	637[a]/673[b]/612[c]	64[a]/2[b]/38[c]	—	—	—	—	—	—	39
NAI-5c	680[a]/703[b]/655[c]	45[a]/1[b]/21[c]	3.1	0.7	—	1.8	(0.67, 0.32)	—	39
NAI-6	565[a]/661[b]	14[a]	14[d]	—	—	—	—	—	40
NAI-7a	597[c]	59.9[c]	3.0	50.7	53.1	23.4	(0.52, 0.47)	0.09	8
NAI-7b	584[c]	78.9[c]	3.0	76.2	79.7	29.2	(0.56, 0.44)	0.17	8
NAI-8a	650[a]	39[c]	4.0	9.6	7.3	9.2	(0.62, 0.38)	0.07	41
NAI-8b	600[a]	73[c]	3.0	49.2	51.4	20.3	(0.54, 0.45)	0.16	41
NAI-9a	588[a]/636[b]/593[c]	26[b]/62[c]	3.3	14.69	10.98	4.80	(0.49, 0.49)	0.15	42
NAI-9b	592[a]/538[b]/555[c]	55[b]/87[c]	3.4	27.95	20.97	7.59	(0.34, 0.59)	0.12	42
NAI-10R	597[c]	39.9[c]	3.4	28.5	28.0	12.4	—	0.07	43
NAI-10S	597[c]	39.9[c]	3.4	28.8	26.6	12.3	—	0.07	43
PDI-1a	620[a]/640[b]	98[a]/38[b]	4	0.065	0.017	0.238	(0.66, 0.33)	—	49
PDI-1b	672[a]/690[b]	54[a]/23[b]	4	0.0375	0.014	0.638	(0.69, 0.29)	—	49
PDI-2c	606[a]/649[b]	34.2[b]	7.5	5.85	2.04	4.93	(0.56, 0.34)	—	50
PDI-3	540[a]	—	3.5	—	—	1.57	—	—	51
PDI-4a	615[a]/626[b]	89[a]	3.68	—	—	—	(0.56, 0.42)	—	52
PDI-4b	579[a]/617[b]	70[a]	3.94	—	—	—	(0.36, 0.33)	—	52
PDI-4c	577[a]/615[b]	6[a]	4.29	—	—	—	(0.37, 0.31)	—	52
PDI-5	650[b]/646[c]	11.5[b]/8.7[c]	2.6	0.05	0.03	0.06	(0.67, 0.32)	—	53
OthI-1a	460[a]	74[a]	—	—	—	11.1	—	—	57
OthI-1b	545[a]	79[a]	2.9	—	—	12.1	—	—	57
OthI-2	664[a]/604[c]	0.5[a]/0.33[b]/61.4[c]	4.1	3.13	2.40	—	(0.60, 0.40)	—	58
OthI-2	—	50[c]	—	7.2	—	3.59	—	—	59
OthI-3	517[a]/510[b]	16.2[a]/95.8[b]	—	—	59.7[d]	24.7[d]	(0.24, 0.49)[d]	0.02	60

[a] Measured in solution. [b] Measured in a neat film. [c] Measured in a co-doped film. [d] Non-doped device.

breakthrough performance with the highest EQE of 24.7%, demonstrating application prospects for this type of aromatic imide/amide.

So far, the application of functionalized imides/amides in OLEDs has been scarcely reported, and the related research still faces some problems to be urgently solved, such as the fluorescence quenching caused by π–π stacking, unsatisfactory EQEs, solution processability and efficiency roll-off. To tackle these issues, the following strategies for molecular structure design would be worth trying.

(a) Various methods can be used to increase the singlet exciton-formation ratio or triplet harvesting, such as TTA, TADF, HLCT and TFDF, to efficiently increase exciton use. The current research studies focused mainly on the combination with TADF to enhance luminescence efficiency. However, TADF materials still suffer from serious efficiency roll-off and instability. Thus, other methods such as TTA, HLCT and TFDF with the adjustment and optimization of molecular structure could be expected to boost the device performance.

(b) Phosphorescence properties may also be used for harvesting triplet excitons. Recent studies have shown that functionalized aromatic imides/amides can exhibit room-temperature phosphorescence by heavy atom substitution[61] or charge-transfer states,[62] and even exhibit transient and persistent mechanoluminescence at room temperature simultaneously which may be used to develop innovative applications in OLEDs.[61]

(c) Combined with the AIE or AIDF effect, the PLQYs and EQEs of aromatic imide/amide-based emitters could be greatly improved to suppress the ACQ phenomenon. Nevertheless, the reported results were not ideal, which should be adjusted further by modifying more suitable groups to balance the conjugation degree and twisted configuration.

(d) Lots of aromatic imide/amide optoelectronic materials are undeveloped as emitters in OLEDs, such as naphthalene diimide,[62] thieno[3,4-*c*]pyrrole-4,6-dione,[63,64] bithiophene imide (BTI),[65,66] and isoindigo.[67,68] BTI has the same heptagonal imide structure as BPI, thus serving as a promising building block of emitters. Additionally, novel aromatic imide/amide systems have to be designed and synthesized to improve luminescence efficiency.

In general, the findings suggest that functionalized imide and amide emitters can exhibit excellent luminescence performances when used in OLEDs by common efforts of organic synthesis chemists and materials scientists.

Conflicts of interest

There are no conflicts to declare.

Acknowledgements

This study was financially supported by the Beijing Natural Science Foundation (No. 2192059) and the University of Chinese Academy of Sciences.

Notes and references

1 C. W. Tang and S. A. VanSlyke, Organic electroluminescent diodes, *Appl. Phys. Lett.*, 1987, **51**, 913–915.
2 X. Cai and S. J. Su, Marching Toward Highly Efficient, Pure-Blue, and Stable Thermally Activated Delayed Fluorescent Organic Light-Emitting Diodes, *Adv. Funct. Mater.*, 2018, **28**, 1802558.
3 Y. Li, J. Y. Liu, Y. D. Zhao and Y. C. Cao, Recent advancements of high efficient donor–acceptor type blue small molecule applied for OLEDs, *Mater. Today*, 2017, **20**, 258–266.
4 Y. Liu, C. Li, Z. Ren, S. Yan and M. R. Bryce, All-organic thermally activated delayed fluorescence materials for organic light-emitting diodes, *Nat. Rev. Mater.*, 2018, **3**, 1–20.
5 D. Ma, Z. Xu, B. Z. Tang and Y. Wang, Recent advances in high performance blue organic light-emitting diodes based on fluorescence emitters, *J. Mater. Chem. C*, 2020, **8**, 2614–2642.
6 H. Sun, L. Wang, Y. Wang and X. Guo, Imide-Functionalized Polymer Semiconductors, *Chem. – Eur. J.*, 2019, **25**, 87–105.
7 T. Yu, L. Liu, Z. Xie and Y. Ma, Progress in small-molecule luminescent materials for organic light-emitting diodes, *Sci. China: Chem.*, 2015, **58**, 907–915.
8 W. Zeng, H. Y. Lai, W. K. Lee, M. Jiao, Y. J. Shiu, C. Zhong, S. Gong, T. Zhou, G. Xie, M. Sarma, K. T. Wong, C. C. Wu and C. Yang, Achieving Nearly 30% External Quantum Efficiency for Orange-Red Organic Light Emitting Diodes by Employing Thermally Activated Delayed Fluorescence Emitters Composed of 1,8-Naphthalimide-Acridine Hybrids, *Adv. Mater.*, 2018, **30**, 1704961.
9 Y. Shi, H. Guo, M. Qin, Y. Wang, J. Zhao, H. Sun, H. Wang, Y. Wang, X. Zhou, A. Facchetti, X. Lu, M. Zhou and X. Guo, Imide-Functionalized Thiazole-Based Polymer Semiconductors: Synthesis, Structure–Property Correlations, Charge Carrier Polarity, and Thin-Film Transistor Performance, *Chem. Mater.*, 2018, **30**, 7988–8001.
10 Y. Shi, H. Guo, M. Qin, J. Zhao, Y. Wang, H. Wang, Y. Wang, A. Facchetti, X. Lu and X. Guo, Thiazole Imide-Based ll-Acceptor Homopolymer: Achieving High-Performance Unipolar Electron Transport in Organic Thin-Film Transistors, *Adv. Mater.*, 2018, **30**, 1705745.
11 Z. Liu, G. Zhang, Z. Cai, X. Chen, H. Luo, Y. Li, J. Wang and D. Zhang, New organic semiconductors with imide/amide-containing molecular systems, *Adv. Mater.*, 2014, **26**, 6965–6977.
12 D. Sun, D. Meng, Y. Cai, B. Fan, Y. Li, W. Jiang, L. Huo, Y. Sun and Z. Wang, Non-Fullerene-Acceptor-Based Bulk-Heterojunction Organic Solar Cells with Efficiency over 7%, *J. Am. Chem. Soc.*, 2015, **137**, 11156–11162.
13 X. Zhang, Z. Lu, L. Ye, C. Zhan, J. Hou, S. Zhang, B. Jiang, Y. Zhao, J. Huang, S. Zhang, Y. Liu, Q. Shi, Y. Liu and J. Yao, A potential perylene diimide dimer-based acceptor material for highly efficient solution-processed non-fullerene organic solar cells with 4.03% efficiency, *Adv. Mater.*, 2013, **25**, 5791–5797.
14 P. K. Samanta, D. Kim, V. Coropceanu and J. L. Bredas, Up-Conversion Intersystem Crossing Rates in Organic Emitters for Thermally Activated Delayed Fluorescence: Impact of the Nature of Singlet *vs.* Triplet Excited States, *J. Am. Chem. Soc.*, 2017, **139**, 4042–4051.
15 C. J. Chiang, A. Kimyonok, M. K. Etherington, G. C. Griffiths, V. Jankus, F. Turksoy and A. P. Monkman, Ultra-high Efficiency Fluorescent Single and Bi-Layer Organic Light Emitting Diodes: The Key Role of Triplet Fusion, *Adv. Funct. Mater.*, 2013, **23**, 739–746.
16 H. Uoyama, K. Goushi, K. Shizu, H. Nomura and C. Adachi, Highly efficient organic light-emitting diodes from delayed fluorescence, *Nature*, 2012, **492**, 234–238.
17 L. Yao, B. Yang and Y. Ma, Progress in next-generation organic electroluminescent materials: material design beyond exciton statistics, *Sci. China: Chem.*, 2014, **57**, 335–345.
18 T. T. Yang, Z. X. Zhou, Y. Zhang, S. W. Liu, Z. G. Chi and J. R. Xu, Recent Advances of Photoluminescence Polyimides, *Acta Polym. Sin.*, 2017, 411–428.

19 Q. Zhang, J. Li, K. Shizu, S. Huang, S. Hirata, H. Miyazaki and C. Adachi, Design of efficient thermally activated delayed fluorescence materials for pure blue organic light emitting diodes, *J. Am. Chem. Soc.*, 2012, **134**, 14706–14709.
20 H. Uoyama, K. Goushi, K. Shizu, H. Nomura and C. Adachi, Highly efficient organic light-emitting diodes from delayed fluorescence, *Nature*, 2012, **492**, 234–238.
21 K. Goushi, K. Yoshida, K. Sato and C. Adachi, Organic light-emitting diodes employing efficient reverse intersystem crossing for triplet-to-singlet state conversion, *Nat. Photonics*, 2012, **6**, 253–258.
22 A. Endo, M. Ogasawara, A. Takahashi, D. Yokoyama, Y. Kato and C. Adachi, Thermally activated delayed fluorescence from Sn^{4+}–porphyrin complexes and their application to organic light emitting diodes—A novel mechanism for electroluminescence, *Adv. Mater.*, 2009, **21**, 4802–4806.
23 W. Li, D. Liu, F. Shen, D. Ma, Z. Wang, T. Feng, Y. Xu, B. Yang and Y. Ma, A twisting donor-acceptor molecule with an intercrossed excited state for highly efficient, deep-blue electroluminescence, *Adv. Funct. Mater.*, 2012, **22**, 2797–2803.
24 W. Li, Y. Pan, L. Yao, H. Liu, S. Zhang, C. Wang, F. Shen, P. Lu, B. Yang and Y. Ma, A hybridized local and charge-transfer excited state for highly efficient fluorescent oleds: molecular design, spectral character, and full exciton utilization, *Adv. Opt. Mater.*, 2014, **2**, 892–901.
25 C. W. Chiu, T. J. Chow, C. H. Chuen, H. M. Lin and Y. T. Tao, Bisindolylmaleimides as red electroluminescence materials, *Chem. Mater.*, 2003, **15**, 4527–4532.
26 Y. S. Lee, Z. Lin, Y. Y. Chen, C. Y. Liu and T. J. Chow, Asymmetric indolylmaleimides as non-dopant type red color emitting dyes, *Org. Electron.*, 2010, **11**, 604–612.
27 W. C. Wu, H. C. Yeh, L. H. Chan and C. T. Chen, Red Organic Light-Emitting Diodes with a Non-doping Amorphous Red Emitter, *Adv. Mater.*, 2002, **14**, 1072–1075.
28 H. C. Yeh, L. H. Chan, W. C. Wu and C. T. Chen, Non-doped red organic light-emitting diodes, *J. Mater. Chem.*, 2004, **14**, 1293–1298.
29 M. E. Jang, T. Yasuda, J. Lee, S. Y. Lee and C. Adachi, Organic Light-emitting Diodes Based on Donor-substituted Phthalimide and Maleimide Fluorophores, *Chem. Lett.*, 2015, **44**, 1248–1250.
30 N. Sharma, S. Kumar, Y. Chandrasekaran and S. Patil, Maleimide–based donor-π-acceptor-π-donor derivative for efficient organic light-emitting diodes, *Org. Electron.*, 2016, **38**, 180–185.
31 N. Venkatramaiah, G. D. Kumar, Y. Chandrasekaran, R. Ganduri and S. Patil, Efficient Blue and Yellow Organic Light-Emitting Diodes Enabled by Aggregation-Induced Emission, *ACS Appl. Mater. Interfaces*, 2018, **10**, 3838–3847.
32 M. Li, Y. Liu, R. Duan, X. Wei, Y. Yi, Y. Wang and C. F. Chen, Aromatic-Imide-Based Thermally Activated Delayed Fluorescence Materials for Highly Efficient Organic Light-Emitting Diodes, *Angew. Chem., Int. Ed.*, 2017, **56**, 8818–8822.
33 M. Li, S. H. Li, D. Zhang, M. Cai, L. Duan, M. K. Fung and C. F. Chen, Stable Enantiomers Displaying Thermally Activated Delayed Fluorescence: Efficient OLEDs with Circularly Polarized Electroluminescence, *Angew. Chem., Int. Ed.*, 2018, **57**, 2889–2893.
34 Y. Danyliv, D. Volyniuk, O. Bezvikonnyi, I. Hladka, K. Ivaniuk, I. Helzhynskyy, P. Stakhira, A. Tomkeviciene, L. Skhirtladze and J. V. Grazulevicius, Through-space charge transfer in luminophore based on phenyl-linked carbazole- and phthalimide moieties utilized in cyan-emitting OLEDs, *Dyes Pigm.*, 2020, **172**, 107833.
35 M. Chapran, R. Lytvyn, C. Begel, G. Wiosna-Salyga, J. Ulanski, M. Vasylieva, D. Volyniuk, P. Data and J. V. Grazulevicius, High-triplet-level phthalimide based acceptors for exciplexes with multicolor emission, *Dyes Pigm.*, 2019, **162**, 872–882.
36 G. Ding, Z. Xu, G. Zhong, S. Jing, F. Li and W. Zhu, Synthesis, photophysical and electroluminescent properties of novel naphthalimide derivatives containing an electron-transporting unit, *Res. Chem. Intermed.*, 2008, **34**, 299–308.
37 Y. Wu, X. Chen, Y. Mu, Z. Yang, Z. Mao, J. Zhao, Z. Yang, Y. Zhang and Z. Chi, Two thermally stable and AIE active 1,8-naphthalimide derivatives with red efficient thermally activated delayed fluorescence, *Dyes Pigm.*, 2019, **169**, 81–88.
38 J. Xiao and Z. Deng, Synthesis and electroluminescent characterization of a symmetric starburst orange-red light material, *J. Lumin.*, 2012, **132**, 2863–2867.
39 S. Luo, J. Lin, J. Zhou, Y. Wang, X. Liu, Y. Huang, Z. Lu and C. Hu, Novel 1,8-naphthalimide derivatives for standard-red organic light-emitting device applications, *J. Mater. Chem. C*, 2015, **3**, 5259–5267.
40 J. A. Gan, Q. L. Song, X. Y. Hou, K. Chen and H. Tian, 1,8-Naphthalimides for non-doping OLEDs: the tunable emission color from blue, green to red, *J. Photochem. Photobiol., A*, 2004, **162**, 399–406.
41 T. Chen, C. H. Lu, C. W. Huang, X. Zeng, J. Gao, Z. Chen, Y. Xiang, W. Zeng, Z. Huang, S. Gong, C. C. Wu and C. Yang, Tuning the emissive characteristics of TADF emitters by fusing heterocycles with acridine as donors: highly efficient orange to red organic light-emitting diodes with EQE over 20%, *J. Mater. Chem. C*, 2019, **7**, 9087–9094.
42 S. Chen, P. Zeng, W. Wang, X. Wang, Y. Wu, P. Lin and Z. Peng, Naphthalimide–arylamine derivatives with aggregation induced delayed fluorescence for realizing efficient green to red electroluminescence, *J. Mater. Chem. C*, 2019, **7**, 2886–2897.
43 Y. F. Wang, H. Y. Lu, C. Chen, M. Li and C. F. Chen, 1,8-Naphthalimide-based circularly polarized TADF enantiomers as the emitters for efficient orange-red OLEDs, *Org. Electron.*, 2019, **70**, 71–77.
44 P. Ganesan, J. Baggerman, H. Zhang, E. J. R. Sudhölter and H. Zuilhof, Femtosecond time-resolved photophysics of 1,4,5,8-naphthalene diimides, *J. Phys. Chem. A*, 2007, **111**, 6151–6156.
45 F. Wurthner, C. R. Saha-Moller, B. Fimmel, S. Ogi, P. Leowanawat and D. Schmidt, Perylene Bisimide Dye Assemblies as Archetype Functional Supramolecular Materials, *Chem. Rev.*, 2016, **116**, 962–1052.

46 F. Wurthner, Perylene bisimide dyes as versatile building blocks for functional supramolecular architectures, *Chem. Commun.*, 2004, 1564–1579.
47 E. H. Beckers, S. C. Meskers, A. P. Schenning, Z. Chen, F. Würthner and R. A. J. Janssen, Charge separation and recombination in photoexcited oligo(*p*-phenylene vinylene):perylene bisimide arrays close to the Marcus inverted region, *J. Phys. Chem. A*, 2004, **108**, 6933–6937.
48 C. Hippius, I. H. van Stokkum, E. Zangrando, R. M. Williams and F. Würthner, Excited State Interactions in Calix[4]arene−Perylene Bisimide Dye Conjugates: Global and Target Analysis of Supramolecular Building Blocks, *J. Phys. Chem. C*, 2007, **111**, 13988–13996.
49 E. Kozma, W. Mróz, F. Villafiorita-Monteleone, F. Galeotti, A. Andicsová-Eckstein, M. Catellani and C. Botta, Perylene diimide derivatives as red and deep red-emitters for fully solution processable OLEDs, *RSC Adv.*, 2016, **6**, 61175–61179.
50 L. Zong, Y. Gong, Y. Yu, Y. Xie, G. Xie, Q. Peng, Q. Li and Z. Li, New perylene diimide derivatives: stable red emission, adjustable property from ACQ to AIE, and good device performance with an EQE value of 4.93%, *Sci. Bull.*, 2018, **63**, 108–116.
51 G. Li, Y. Zhao, J. Li, J. Cao, J. Zhu, X. W. Sun and Q. Zhang, Synthesis, Characterization, Physical Properties, and OLED Application of Single BN-Fused Perylene Diimide, *J. Org. Chem.*, 2015, **80**, 196–203.
52 R. K. Gupta, D. Das, P. K. Iyer and A. S. Achalkumar, First Example of White Organic Electroluminescence Utilizing Perylene Ester Imides, *ChemistrySelect*, 2018, **3**, 5123–5129.
53 S. Dayneko, M. Pahlevani and G. C. Welch, Solution Processed Red Organic Light-Emitting-Diodes using an N-Annulated Perylene Diimide Fluorophore, *J. Mater. Chem. C*, 2020, **8**, 2314–2319.
54 Q. Liu, S. E. Bottle and P. Sonar, Developments of Diketopyrrolopyrrole-Dye-Based Organic Semiconductors for a Wide Range of Applications in Electronics, *Adv. Mater.*, 2020, **32**, 1903882.
55 V. Cuesta, M. Vartanian, P. Malhotra, S. Biswas, P. de la Cruz, G. D. Sharma and F. Langa, Increase in efficiency on using selenophene instead of thiophene in π-bridges for D-π-DPP-π-D organic solar cells, *J. Mater. Chem. A*, 2019, **7**, 11886–11894.
56 X. Song, N. Gasparini, M. M. Nahid, S. H. K. Paleti, C. Li, W. Li, H. Ade and D. Baran, Efficient DPP Donor and Nonfullerene Acceptor Organic Solar Cells with High Photon-to-Current Ratio and Low Energetic Loss, *Adv. Funct. Mater.*, 2019, **29**, 1902441.
57 P. Data, A. Kurowska, S. Pluczyk, P. Zassowski, P. Pander, R. Jedrysiak, M. Czwartosz, L. Otulakowski, J. Suwinski, M. Lapkowski and A. P. Monkman, Exciplex Enhancement as a Tool to Increase OLED Device Efficiency, *J. Phys. Chem. C*, 2016, **120**, 2070–2078.
58 Y. Wang, J. Zhou, X. Wang, X. Zheng, Z. Lu, W. Zhang, Y. Chen, Y. Huang, X. Pu and J. Yu, An efficient guest/host fluorescent energy transfer pair based on the naphthalimide skeleton, and its application in heavily-doped red organic light-emitting diodes, *Dyes Pigm.*, 2014, **100**, 87–96.
59 J. Zhou, P. Chen, X. Wang, Y. Wang, Y. Wang, F. Li, M. Yang, Y. Huang, J. Yu and Z. Lu, Charge-transfer-featured materials—promising hosts for fabrication of efficient OLEDs through triplet harvesting via triplet fusion, *Chem. Commun.*, 2014, **50**, 7586–7589.
60 Z. Huang, Z. Bin, R. Su, F. Yang, J. Lan and J. You, Molecular Design for Non-Doped OLEDs Based on a Twisted Heptagonal Acceptor: Delicate Balance between Rigidity and Rotatability, *Angew. Chem., Int. Ed.*, 2020, DOI: 10.1002/anie.201915397.
61 J. A. Li, J. Zhou, Z. Mao, Z. Xie, Z. Yang, B. Xu, C. Liu, X. Chen, D. Ren, H. Pan, G. Shi, Y. Zhang and Z. Chi, Transient and Persistent Room-Temperature Mechanoluminescence from a White-Light-Emitting AIEgen with Tricolor Emission Switching Triggered by Light, *Angew. Chem., Int. Ed.*, 2018, **57**, 6449–6453.
62 S. Kuila, A. Ghorai, P. K. Samanta, R. B. K. Siram, S. K. Pati, K. S. Narayan and S. J. George, Red-Emitting Delayed Fluorescence and Room Temperature Phosphorescence from Core-Substituted Naphthalene Diimides, *Chem. – Eur. J.*, 2019, **25**, 16007–16011.
63 Q. Liao, K. Yang, J. Chen, C. W. Koh, Y. Tang, M. Su, Y. Wang, Y. Yang, X. Feng, Z. He, H. Y. Woo and X. Guo, Backbone Coplanarity Tuning of 1,4-di(3-alkoxy-2-thienyl)-2,5-difluorophenylene-Based Wide Bandgap Polymers for Efficient Organic Solar Cells Processed from Nonhalogenated Solvent, *ACS Appl. Mater. Interfaces*, 2019, **11**, 31119–31128.
64 C. E. Song, H. Ham, J. Noh, S. K. Lee and I. N. Kang, Efficiency enhancement of a fluorinated wide-bandgap polymer for ternary nonfullerene organic solar cells, *Polymer*, 2019, **188**, 122131.
65 X. Guo, R. P. Ortiz, Y. Zheng, Y. Hu, Y. Y. Noh, K. J. Baeg, A. Facchetti and T. J. Marks, Bithiophene-Imide-Based Polymeric Semiconductors for Field-Effect Transistors: Synthesis, Structure−Property Correlations, Charge Carrier Polarity, and Device Stability, *J. Am. Chem. Soc.*, 2011, **133**, 1405–1418.
66 Y. Shi, H. Guo, M. Qin, Y. Wang, J. Zhao, H. Sun, H. Wang, Y. Wang, X. Zhou and A. Facchetti, Imide-Functionalized Thiazole-Based Polymer Semiconductors: Synthesis, Structure–Property Correlations, Charge Carrier Polarity, and Thin-Film Transistor Performance, *Chem. Mater.*, 2018, **30**, 7988–8001.
67 M. Li, Z. Qiu, G. Zhang, Y. Liu, L. Xiong, D. Bai, M. Zhu, Q. Peng and W. Zhu, Efficient chemical structure and device engineering for achieving difluorinated 2,2′-bithiophene-based small molecular organic solar cells with 9.0% efficiency, *J. Mater. Chem. A*, 2018, **6**, 12493–12505.
68 J. Miao, B. Meng, J. Liu and L. Wang, An A–D–A′–D–A type small molecule acceptor with a broad absorption spectrum for organic solar cells, *Chem. Commun.*, 2018, **54**, 303–306.

